

The Detector Assembly and the Ultra Low Temperature Refrigerator for XRS

F. Scott Porter^{a*}, Michael D. Audley^b, Regis P. Brekosky^{d,a}, Rebecca J. Derro^a, Michael J. Dipirro^a, Keith C. Gendreau^{c,a}, John D. Gygas^{d,a}, Richard L. Kelley^a, Dan McCammon^c, Armando Morell^a, Scott D. Murphy^{f,a}, Robert J. Paulos^c, Thai Pham^a, Caroline K. Stahle^a, Andrew E. Szymkowiak^a, and James G. Tuttle^a

^aNASA/Goddard Space Flight Center, Greenbelt, MD, USA

^bInstitute of Space and Astronautical Science, Sagami-hara, Kanagawa, Japan

^cUniversity of Maryland, College Park, MD, USA

^dSwales and Associates, Beltsville, MD, USA

^eUniversity of Wisconsin, Madison, WI, USA

^fRocket Science, Inc., Ellicott City, MD, USA

ABSTRACT

The X-ray spectrometer (XRS) on the Japanese Astro-E observatory is the first ultra low temperature space borne instrument. The system utilizes a 900g ferric ammonium alum (FAA) adiabatic demagnetization refrigerator (ADR) with ³He gas gap heat switch to cool the detector assembly to 0.060 K. The system operates in a "single shot" configuration allowing the system to remain at its operating temperature for about 40 hours in the lab before executing a recharge cycle. The on-orbit performance is expected to be about 36 hours with a 97% duty cycle. The detector assembly for XRS consists of a 32 channel microcalorimeter array, bias electronics, thermometry, and an anti-coincidence detector that are attached to the cold stage of the ADR. To thermally isolate the detector system from the superfluid helium reservoir, the detector system is suspended by Kevlar¹ cords and electrical connection is made by 130, 20 micron diameter, tensioned NbTi leads. The detectors are read out in a source-follower arrangement using FET amplifiers operating at 130 K mounted in nested, thermally-isolated assemblies that also use Kevlar suspension and stainless steel wiring. The design and thermal performance of this system will be discussed.

Keywords: X-ray, Calorimeter, ADR, XRS, ASTRO-E, Low Temperature

1. INTRODUCTION

The XRS instrument is the high resolution x-ray spectrometer for the Japanese Astro-E spacecraft that will be launched in early 2000. The instrument was developed as a collaboration between NASA/GSFC, the Institute of Space and Astronautical Science (ISAS), the University of Wisconsin, and Sumitomo Heavy Industries. The primary goal of the instrument is to produce high-resolution x-ray spectra of astrophysical plasmas, allowing detailed plasma diagnostics including temperature, composition, ionization state, and velocity diagnostics of emission lines. An overview of the entire instrument and its mission can be found in Kelley et al².

The detector system of the XRS consists of an x-ray microcalorimeter array, a technology that we pioneered at Goddard Space Flight Center along with our collaborators at the University of Wisconsin. We have previously flown this type of detector system three times on a sub-orbital sounding rocket with great success³, but the XRS represents the first time that this technology has been deployed on a satellite. The XRS microcalorimeter detector senses the incident x-ray energy by measuring the heat deposited in a very low heat capacity absorber with a very high responsivity thermometer. Using this method we can achieve resolving powers near 1000 with unit quantum efficiency in a broad band from <400 eV to ~12 keV. A detailed description of the flight detector array can be found in Stahle et al., and a description of the performance and calibration can be found in Gendreau et al. Briefly, however, the XRS microcalorimeter array consists of 32 micromachined silicon pixels which are suspended and thermally isolated by thin silicon beams from a monolithic frame. The thermometers are ion implanted thermistors whose resistance is governed by hopping conduction. The absorbers are thin wafers of HgTe, a semi-metal which is a compromise between good thermalization and a high Debye temperature. The individual absorbers are

* Correspondence: Email: Frederick.S.Porter@gsfc.nasa.gov

epoxied to a silicon spacer and then to the pixel body producing a composite x-ray microcalorimeter. This is essentially the same technique that was successfully deployed on our sounding rocket experiment. The XRS microcalorimeter array is a "bilinear" device consisting of two parallel 18 element rows which are staggered to interleave their supporting structures. However only 16 pixels in each row are instrumented.

The high resolving power achieved with the x-ray microcalorimeter does come with a price in the complexity of the instrument. In order to produce the high responsivity of the thermometer, the low heat capacity of the pixels, low Johnson noise, and low thermal fluctuation noise, the detectors must be run at very low temperatures. The XRS microcalorimeter array is operated at 60 mK, a feat only previously achieved in space by our sounding rocket experiment. The XRS refrigerator which produces a stable 60 mK temperature stage and the detector Front End Assembly (FEA) are the subjects of this paper.

The XRS low temperature stage uses an adiabatic demagnetization refrigerator (ADR), a technique described in more detail in section 2, but that essentially involves aligning a spin system in a paramagnet with an external field and then demagnetizing the system, which absorbs heat to maintain constant entropy. Prior to the 1960's and the large-scale availability of ³He, this was the only way to reach millikelvin temperatures. However, the ADR is essentially ideal for space applications since it requires neither complicated gas handling systems nor gravity to operate. The limiting factor for this technology is that, compared to modern laboratory refrigerators, the cooling power is very small and the refrigerator is essentially a single shot device which must be periodically recharged. In the XRS implementation, the ADR absorbs about 3.2 μW at 60 mK for 40 hours before requiring a one hour recharge cycle. The XRS ADR is by far the largest refrigerator of its type ever built consisting of almost 1 kg of active refrigerant.

The Front End Assembly on the XRS consists of the microcalorimeter array and anti-coincidence detector, their temperature controlled stage, thermometry, thermal attachment to the ADR, bias electronics, FET trans-impedance amplifiers, and the first two infrared blocking filters. The FEA is modular with replaceable FET amplifier assemblies and bias electronics, but assembles into a removable unit that attaches to the XRS helium tank and the ADR. A detailed description of this system is in section 3. Briefly, the detector stage is suspended from its 1.3K housing by Kevlar cords and electrical connection is made using 20 um diameter CuNi clad NbTi superconducting wire. The end result is that the heat load on the detector stage is only 0.3 μW at 60 mK, 10% of the total parasitic heat load on the ADR. This is almost entirely due to the wiring layer since the detector bias power is negligible. The gas gap heat switch dominates the balance of the ADR's parasitic heat load with a small addition from its Kevlar suspension and cosmic ray deposition in orbit.

1.1 Overview of the XRS cryostat

The focus of this paper is a description of the XRS low temperature refrigerator and the Front End Assembly, however a brief outline of the XRS cryostat assembly will help put this information in context. More information on the XRS helium insert can be found in Breon *et al.*⁴

The XRS cryostat is a dual cryogen system with an outer 130 liter solid neon tank at 17K, and an inner 30 liter superfluid helium tank at 1.3K. An overview of the thermal stages and their nominal heat loads is shown in Table 1. Two competing requirements drove the design of the XRS cryostat. The first was the severe weight and size constraints imposed by the Astro-E spacecraft, where the XRS is only one of three instruments on the X-ray observatory. The second requirement was that the instrument should have a two year lifetime. The first requirement lead to the minimal cryogen loads described above; the challenge was how to keep the parasitic heat loads small enough to achieve a two year lifetime. The lifetime requirement is severe, giving a maximum parasitic heat load on the helium tank of 1.3 mW. This can be compared to a "good" laboratory cryostat that typically has a parasitic heat load of between 100-200 mW without instrumentation. Thus the designs of every other component of the instrument, including the ADR and FEA, were constrained by the fact that even a small amount of heat significantly impacts the life of the instrument. As can be seen in Table 1, the performance of the helium insert exceeded the minimum acceptable level by almost a factor of two.

Table 1. Nominal parasitic heat loads and operating temperatures for the XRS cryostat

Thermal Stage	Operating temp.	Parasitic heat load
Dewar main shell	250 K	--
Solid Ne tank	17K	~1 W
Superfluid He tank	1.3K	0.7 mW
ADR	60 mK	3.2 μW

The superconducting magnet for the ADR is mounted in the helium tank and is wired with high-T_c superconducting leads. The maximum current for the magnet is only 2A with a central field of 20 kG. This minimizes the heat load from the

normal metal stage of the magnet leads on the neon tank. The ADR is mounted in the 3.13" diameter, 11" long magnet bore and is suspended by Kevlar cords from the helium tank. The FEA then caps the magnet bore and the central detector stage is separately suspended from the helium tank making thermal contact to the ADR with annealed gold foils.

The microcalorimeter arrays are thermal devices, so they have both a bolometric as well as a calorimetric response. Thus they require extensive thermal shielding while still providing an aperture for x-rays to enter the cryostat. To set the scale, the bias power dissipates 0.2 pW/pixel that significantly heats each detector element. To combat the bolometric effect, the XRS employs a series of five infrared blocking filters, one at each thermal stage in the cryostat. The filters are extremely thin, ~1000 Å of polyimide, with a 1000 Å aluminum coating which is sufficient to block the bolometric response of the detectors while still allowing broad band x-ray transmission. A description of the XRS filters and their calibration can be found in Audley *et al.*⁵

Thus, the XRS is a complex low temperature instrument that employs several technologies that are first-of-their-kind on a satellite. For example, the XRS is the first microcalorimeter instrument, the first ADR, the longest lifetime cryostat, the coldest refrigerator, and the highest resolving power broadband x-ray telescope on a satellite!

2. THE ADIABATIC DEMAGNETIZATION REFRIGERATOR (ADR)

2.1 Overview and Principle of Operation

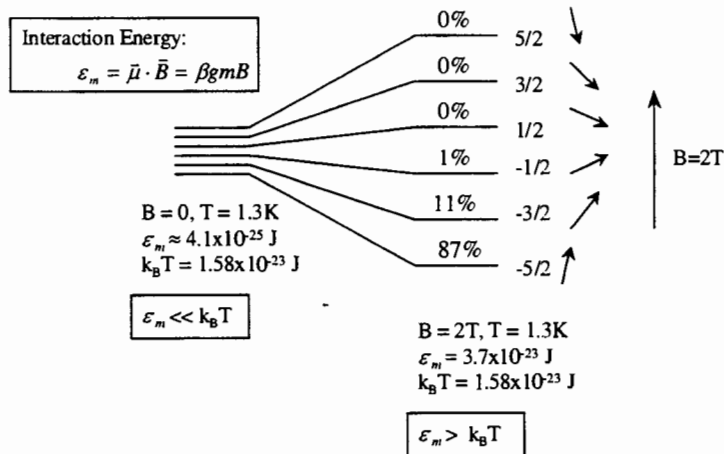


Figure 1. Schematic energy diagram of the magnetic ions in an FAA salt. The left side depicts the degenerate energy levels at 1.3 K, B=0, and the right shows the occupation of the energy levels at 1.3K, B=2T.

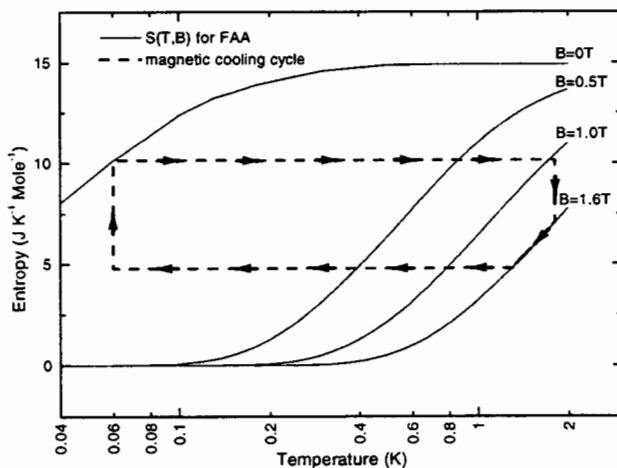


Figure 2. Entropy vs temperature curves for FAA in various external fields^{6,7}. The magnetic cooling cycle is also shown as the dashed lines with arrows. During the cycle the salt is magnetized to an average field of 1.6T at 1.8K and then allowed to cool to 1.3K before it is adiabatically demagnetized to 0.0585 K. The salt then trades entropy against the parasitic heat load until it reaches B=0 at which point it is adiabatically remagnetized to 1.8K and the cycle is repeated.

The Adiabatic Demagnetization Refrigerator on XRS consists of several key components: the magnet which is integral to the cryostat, the heat switch to the helium bath, the salt pill (refrigerant), and the suspension system. The basic requirement for the refrigerator is to maintain a stable 60.00 mK platform for the microcalorimeter detectors with at least a 90% duty cycle. The refrigerator itself is based on a magnetic cooling technique that was largely abandoned by the low temperature community with the widespread availability of ^3He and dilution refrigerators in the late 1960's. However, an ADR does not require gravity, a complicated gas-handling system, or moving parts to operate, making it nearly ideal as a space based refrigerator. The technology is also reappearing in the laboratory where small, turnkey cryogenic systems are becoming more commonplace for applications in non-traditional fields such as commercial materials characterization. The downsides of the technology are that it has a very small cooling power compared to even a small dilution refrigerator and it is a single shot device requiring periodic recharging.

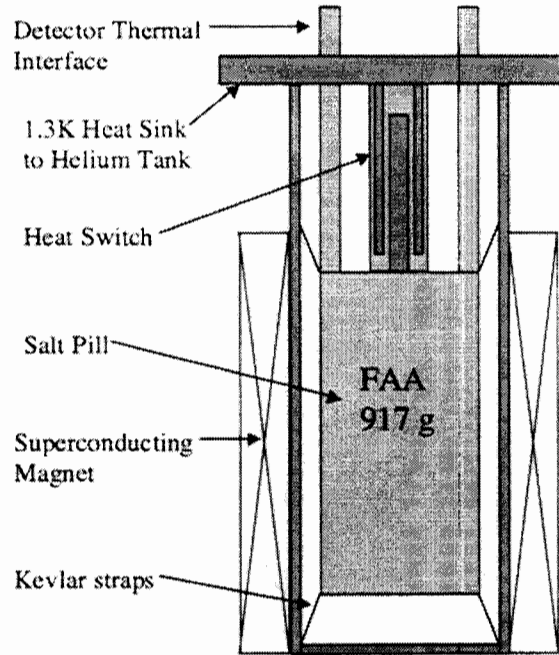


Figure 3. Schematic overview of an Adiabatic Demagnetization Refrigerator (ADR).

Invented in the late 1920's, the central refrigerant in an ADR is a paramagnetic salt, where ions with a dipole magnetic field are spaced far apart to achieve a very low ordering temperature. In the XRS salt pill we have used the compound ferric ammonium alum (FAA) with the chemical formula:



which was first used as a magnetic refrigerant in the 1930's. The 12 waters of hydration per molecule serve to keep the magnetic iron atoms very well separated giving an ordering temperature of about 26 mK⁷. Above the ordering temperature, the magnetic salt behaves like an ideal, isolated spin system with a total angular momentum of 5/2 and a Lande g factor of 2.0. A total angular momentum of 5/2 gives 6 possible electronic spin configurations as shown in figure 1. At moderate temperatures well above the ordering temperature, all six states are degenerate and the entropy of the system is simply

$$S = Nk_B \ln 6, \quad (2)$$

where N is the total number of molecules in the refrigerant. If we now apply a field to the paramagnetic salt, we can break the degeneracy in the electronic configuration and artificially lower the entropy of the spin system. This produces a heat of magnetization because of the interaction energy:

$$\epsilon_m = \vec{\mu} \cdot \vec{B} = \beta g m B \quad (3)$$

where the external field performs work on the spin system. In a standard ADR the heat of magnetization is conducted away to the liquid helium bath through a heat switch. If we then isolate the paramagnetic salt by opening the heat switch and then reduce the applied magnetic field, the adiabatic system must lower its temperature to compensate and maintain a constant entropy. This is shown in Figure #2. Completely demagnetizing the paramagnet will allow the system to reach equilibrium at a temperature compatible with the zero field entropy. The system will then warm at a rate determined by the heat capacity and the parasitic heat load. However, if we only partially demagnetize the system to a moderate temperature we can then maintain that temperature by trading residual field and entropy against the parasitic heat load. When we have exhausted the residual field on the salt pill we then adiabatically re-magnetize the salt pill back to the helium bath temperature and then use the heat switch to again artificially suppress the entropy. The entire cycle is shown in figure #2. The hold time of the refrigerator is then limited by the efficiency (theoretically reaching 100% of Carnot) and the parasitic heat load.

A schematic overview of the XRS ADR is shown in Figure #3. The suspension system is braided kevlar cord tensioned at both ends of the salt pill with the axial load taken up by the heat switch housing. Both the heat switch and the salt pill were recently redesigned and are described in more detail below.

2.2 The XRS Gas Gap Heat Switch

The XRS heat switch is a ^3He gas gap design shown in Figure #4. In this design, gas conduction between a series of re-entrant copper cylinders links the salt pill to the helium bath. This transports the heat of magnetization from the salt pill to the thermal sink. Adsorbing the gas onto a Zeolite getter opens the heat switch allowing the salt pill to be isolated from the helium bath. However, the gas gap heat switch remains mechanically attached to the salt pill, limiting the on/off ratio that limits the hold time. In the XRS design, the parasitic off conductance of the heat switch is about $2.6 \mu\text{W}$ which dominates the total $\sim 3.2 \mu\text{W}$ on the salt pill, and drives the size of the salt pill as discussed in section 2.3. The on conductance of the salt pill is driven by the need to achieve a high duty cycle and limit the contribution of the refrigerator to the lifetime of the helium bath.

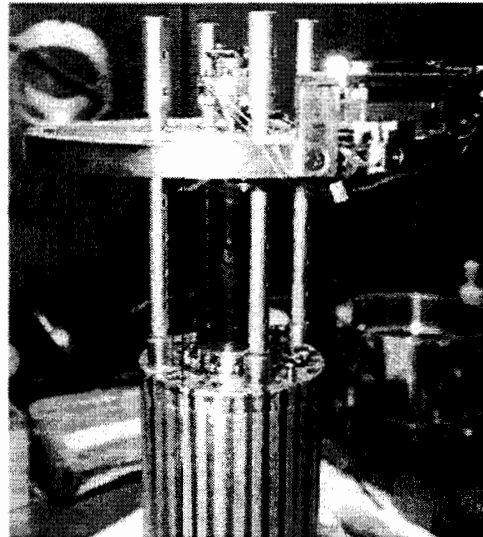
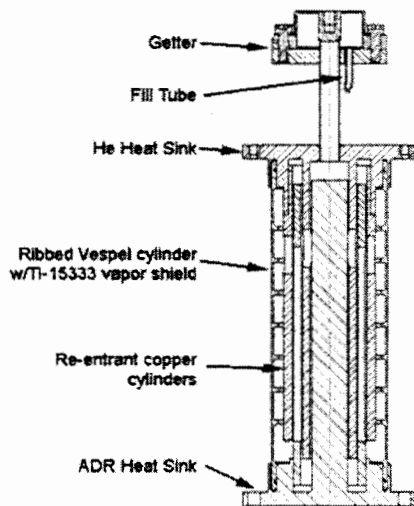


Figure 4. (left) Cross Section of the Gas Gap Heat switch. (right) Heat switch mounted on salt pill in a partially assembled ADR.

The XRS gas gap heat switch was re-designed in 1998 to achieve greater mechanical margin, concentrating on the reliability of joints and control in the alignment process. As shown in Figure 4, the heat switch is constructed from two re-entrant cylindrical copper endpieces that form the thermal anchors for the salt pill and the helium bath. The mechanical link between the two ends is then made with a Vespel[®] SP-1 outer shell 0.020" thick and ribbed on the interior for stiffness. Vespel, however, is porous to He at room temperature thus allowing the switch to de-pressurize over time. To allow the switch to survive long storage periods, a vapor barrier is epoxied to the exterior of the Vespel cylinder. The vapor barrier used is a 0.005" thick foil of TI-15333⁹, a titanium alloy with a thermal conductivity 10 times lower than stainless that is not porous to helium.

The on-conduction of the heat switch is a function of the surface area of the re-entrant cylinders and the gap between them and is only weakly dependent on the gas pressure for transition flow transport (the switch pressure at ~ 1 torr is between molecular and viscous flow). The nominal gap between the cylinders in the XRS design is 0.010" and is set using a five axis alignment jig. The Vespel outer cylinder is then epoxied to the copper end pieces using ScotchWeld¹⁰ 2216. The getter assembly contains a stainless steel connecting tube, which provides thermal isolation from the helium bath, and is vacuum brazed to both the getter base and the upper copper end piece as shown in Figure 3. An upper aluminum cup which holds the Zeolite getter material is attached with an indium o-ring. The thermal conductance between the getter and the 1.3 K heat sink is tuned by gold plating the stainless steel connecting tube and then stripping the gold from part of its length. The ^3He is filled through a Be-Cu fill tube and a soft soldered stainless steel pinch tube. The getter material is thermally anchored inside the getter cup using a high temperature cure silver filled epoxy.

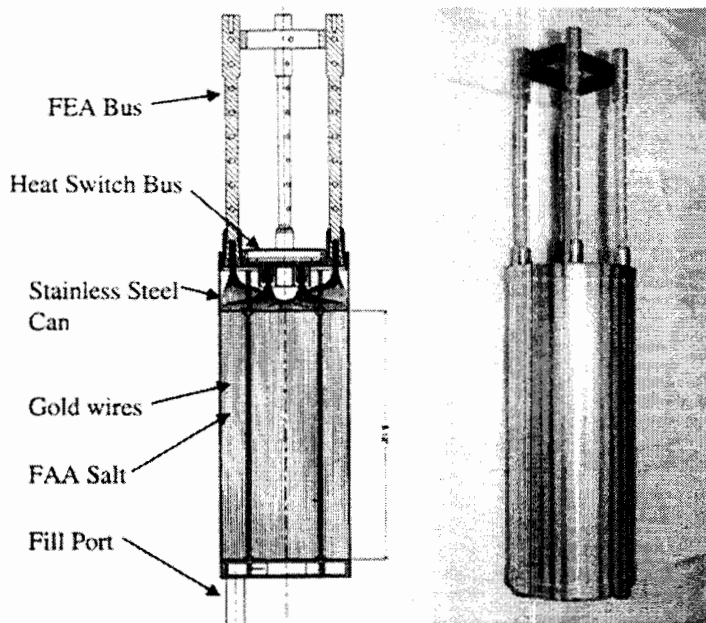


Figure 5. (left) Schematic cross section of the XRS flight salt pill. (right) Side view of the XRS flight salt pill

^3He is used as the exchange gas in the switch instead of ^4He for several important reasons. It does not form a superfluid film in the temperature range at which the switch operates (0.060-1.8K), avoiding superfluid shorts under the vapor barrier. In previous switches small pockets of ^4He had formed under the vapor barrier causing thermal shorts due to transport in the superfluid film. In addition, the lower binding energy of ^3He to Zeolite allows the getter to be operated at a lower temperature (currently ~ 14 K, although the switch is fully conducting around 9 K), lowering the conducted heat to the helium bath. The switch is evacuated at room temperature and then backfilled with ^3He .

The fully constructed heat switch has an on-conductance of ~ 70 mW/K at 1.8K and an off conductance of $2.6 \mu\text{W}$ at 0.060 K giving an on/off ratio of 2.7×10^4 . This allows the salt pill to achieve a hold time of 40 hours at 60 mK in ground testing with a 1 hour recharge time giving a 97% duty cycle. The flight and flight spare heat switches have, however, had a time dependent performance degradation which is consistent with a gradually contaminating getter. This makes the heat switch difficult to turn off after the initial cooldown from room temperature. This effect has been successfully annealed out in each cooldown cycle in both the flight and flight spare heat switches after which both switches perform nominally. This effect is probably related to insufficient bake-out and pump-out of the switch body during assembly. A second flight spare heat switch has been produced using more rigorous bake-out procedures and is currently under test. No degradation in the getter performance has yet been observed.

2.3 The XRS FAA salt pill

The XRS ADR program was a central driver for the resurgence of paramagnetic refrigerators for both spaceflight and ground use after they were essentially supplanted by dilution refrigerators at the end of the 1960's. The initial designs were for a G10 outer can with a common gold wire thermal bus terminating into a copper thermal anchor for both the Front End Assembly (FEA) and the heat switch. After concerns about the mechanical reliability of the G10-epoxy construction of the salt pill, the

salt pill was re-designed in 1997 in a collaboration between NASA/GSFC and the University of Wisconsin and was built at the Space Sciences Engineering Center at the University of Wisconsin. The new design incorporated advancements that had been made by other groups¹¹ who were now actively pursuing ADRs for both ground and space application.

Table #2. Summary of the XRS salt pill parameters

Total mass of FAA salt	918.6 g (1.91 moles)
Total salt pill mass	1729.6 g
Average density of salt	> 99.0% of bulk crystalline density
Number of gold wires in heat switch bus	800
Number of gold wires in FEA buses (total)	800
Cooling capacity	0.491 J @ 63.5 mK
	0.42 J @ 58.5 mK
Heat switch bus thermal cond. at 65 mK	3.0 mW/K
“ “ “ at 1.8K	350 mW/K
Total FEA bus thermal cond. at 65 mK	3.6 mW/K

A summary of the salt pill characteristics is shown in Table 2. The new ADR design, shown in figure 5, is constructed from a stainless steel outer can with brazed copper thermal anchors for the FEA detector stage and the heat switch. Except for the thermal anchors all other joints in the outer can were welded stainless steel giving the salt pill a large margin against rupture either from thermal stress in the housing or from the salt. The principal concern is that the extremely hydrated FAA salt decomposes if the water is allowed to evaporate through an imperfection in the housing. Dehydration effectively decreases the ADR cooling capacity over time, and decreases thermal contact between the salt and the thermal buses. Stainless steel, however, has been shown to have a Schottky heat capacity anomaly at ~ 70 mK¹². This causes the thermal time constant of the stainless steel housing to increase dramatically at low temperatures as the heat capacity increases and the thermal conductivity drops. The additional heat capacity of the shell does not contribute significantly to the heat capacity of the ADR but the additional time dependent heat load from the stainless steel shell being out of thermal equilibrium with the salt during the initial demagnetization could substantially decrease the cooling power. The XRS design overcomes this problem by electroplating 0.003” thick copper stripes, over-plated with gold, along the axial length of the salt pill and thermally connecting them to the salt through the heat switch thermal bus. Narrow stripes were used to limit eddy current losses. This proved an effective method of keeping the entire salt pill in thermal equilibrium during demagnetization. This is shown in Figure 6, where the far end of the salt pill, which is the least thermally connected, is at most 10 mK above the salt temperature.

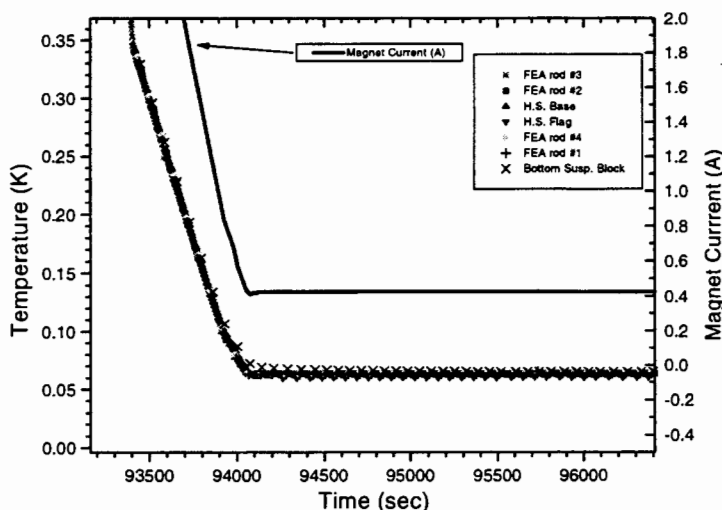


Figure 6. The XRS salt pill approaching tight temperature control at 65 mK. Note that all 7 thermometers on the salt pill are almost in equilibrium during demagnetization including the “Bottom Susp. Block” which is at the far end of the salt pill.

The new salt pill design also incorporates two separate thermal buses to optimize the two main modes of operation for the salt pill: absorbing heat at low temperatures, and expelling the heat of magnetization during recharge. The parasitic heat load from the FEA calorimeter thermal stage (CTS) is $0.24 \mu\text{W}$ and the detector stage is temperature controlled at 60.00

mK by regulating the magnetic field on the salt pill. However the thermal conductivity between the CTS and the salt pill thermal bus is only 0.14 mW/K, forcing the thermal bus to run at 58.3 mK to control the CTS temperature at 60 mK. However, if the heat switch is connected to the same thermal bus then its large parasitic heat load of 2.6 μ W would dominate the total heat flowing from the thermal bus to the salt. The thermal connection to the salt is dominated by the boundary resistance between the gold wire thermal bus and the FAA salt. If the heat load is large then a large number of gold wires are required to keep a large gradient from developing between the thermal bus and the salt and thus requiring the salt to run at a lower temperature with an inherent loss of efficiency. Early designs required up to 5000 gold wires in the thermal bus to accomplish this feat. In the new salt pill design, the heat switch was separated onto its own thermal bus since the temperature of the heat switch thermal bus is irrelevant while the heat switch is off. This allows the two thermal buses to be optimized separately, and the salt itself to run at a temperature closer to the CTS temperature and at greater efficiency. The thermal conductivity of the two thermal buses is shown as a function of temperature in figure 7. At 60 mK the thermal conductivity of the FEA thermal bus to the salt was measured at 3 mW/K. This implies a salt temperature of 58.2 mK to maintain the bus interface at 58.3 mK and the CTS temperature at 60.0 mK. Figure 7 also shows the thermal conductivity of the heat switch thermal bus to the salt as 2.5 mW/K at 60 mK. Thus the heat switch interface with 2.6 μ W of parasitic power plus 0.4 μ W from the kevlar suspension and ancillary electrical leads runs at 59.5 mK. The result is a few percent increase in efficiency. However, the thermal conduction of the completed salt pill buses exceeded their design goal by a factor of two so the effect was expected to be more pronounced.

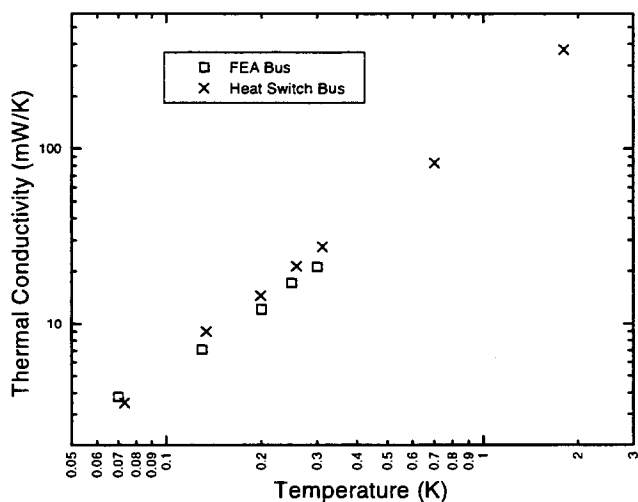


Figure 7. The thermal conductivity of the FEA thermal bus and the heat switch thermal bus to the FAA salt.

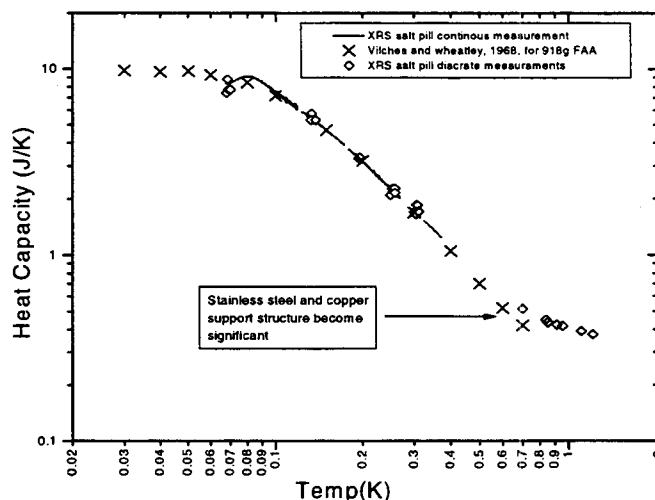


Figure 8. The heat capacity of the XRS salt pill compared to the classic measurement by Vilches and Wheatley⁷.

2.4 ADR performance

The total parasitic heat load on the salt pill is 3.2 μ W from the CTS (detector stage), the kevlar suspension, wiring, and heat switch. The total cooling capacity of the ADR with a 20 kG central field, and a 15.9 kG average field, has been measured at 0.49 J at 63.5 mK and 0.42 J at 58.5 mK. The calculated cooling capacity of the salt pill at 63.5 mK is 0.63 J using $S(B=0,T)$ from Vilches and Wheatley⁷ and $S(B,T)$ from a Brillouin⁶ function of B/T . The heat capacity of the salt pill is shown in Figure 8 and compares favorably to the measurements of Vilches and Wheatley⁷. This shows that the salt pill is fully hydrated and thermally well connected. Two salt pills of this type have been fabricated to date. The flight model is integrated and performing nominally on the spacecraft. The hold time in its flight configuration is 40 hours at 58.5 mK (detector stage controlled at 60.0 mK), and is expected to be 36 hours in flight due to a 0.3 μ W additional heat load from cosmic rays. The heat evolved from the salt pill during magnetization at 1.8 K is calculated to be 10.5 J with another 6.5 J used to cool the salt pill to 1.35 K before demagnetization. This gives a total of 17 J expelled from the salt pill during the recycle process. The efficiency at 63.5 mK is then 2.8 % compared to the calculated value of 3.6%, and the Carnot efficiency from 1.8K to 63.5 mK of 3.7%. We are thus achieving 78% of the Carnot efficiency, with small losses due to eddy current heating, self shielding of the salt, and non-isothermal cooling.

Finally, the flight spare salt pill has completed its laboratory testing and has a cooling capacity that is less than 1% different from the flight model. This shows that the salt pill construction is very reproducible.

3. THE FRONT END ASSEMBLY (FEA)

The XRS Front End Assembly (FEA) contains most of the low temperature thermal and electrical support systems for the microcalorimeter detector array. An overview of the FEA is shown in Figures 9 and 10. The FEA was designed to make the microcalorimeter system modular and easily removable from the cryostat. This was important during test and integration when various detector components were tested and replaced. The central section of the FEA contains the microcalorimeter array and an anti-coincidence detector mounted in a light tight copper box referred to as the Calorimeter Thermal Stage (CTS) that is thermally anchored to the ADR. The thermal attachment to the ADR, however, is made with annealed gold foils allowing the CTS to be separately suspended inside the FEA with Kevlar cords. This allows the detector system to be assembled and tested and later mounted to the flight ADR.

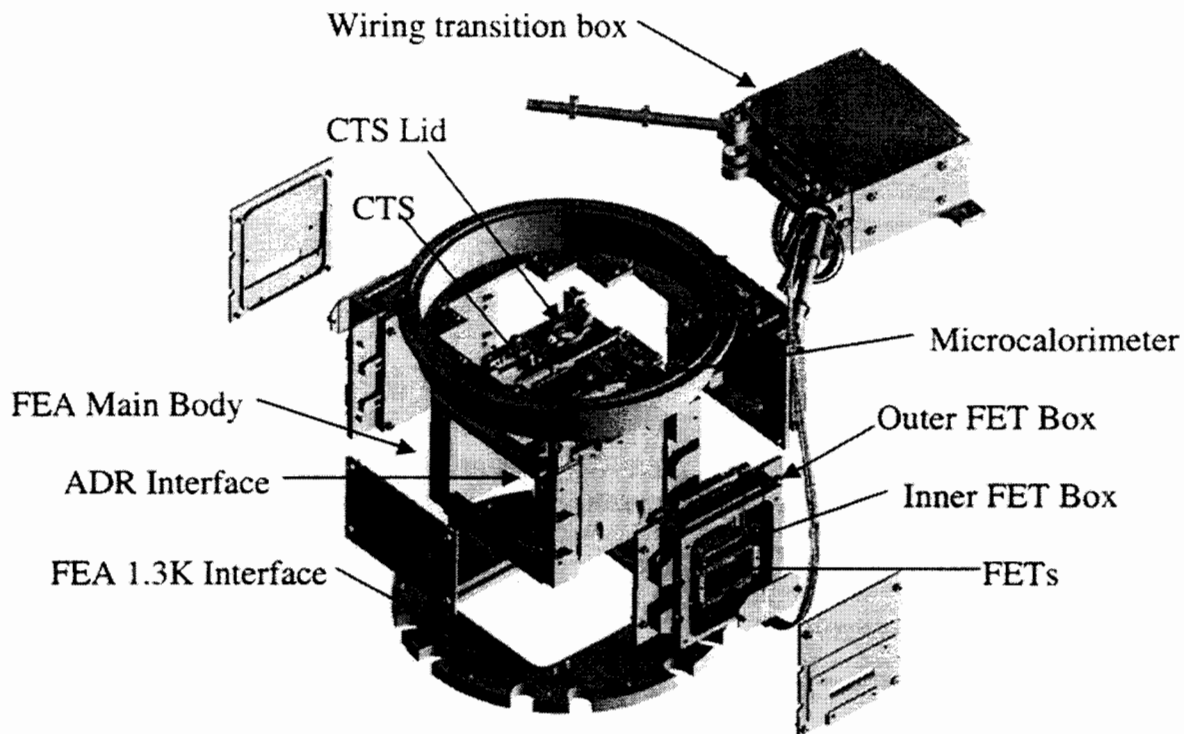


Figure 9. Exploded view of the XRS Front End Assembly (FEA).

The FEA also houses the first stage electrical read-out of the microcalorimeters and the anti-coincidence detector. An overview of the first stage-read-out is shown in Figure 11. The circuit is basically a FET source-follower trans-impedance amplifier with nearly unit gain. The goal is to reduce the $10\text{ M}\Omega$ source impedance of the microcalorimeter detectors (under bias) so that standard flexible cables can route the signals through the rest of the cryostat. The high source impedance forces the wiring between the detectors and the FETs to be very stiff to avoid microphonics. An additional complication is that the FETs are operated at 130 K to minimize their noise contribution to the read-out signal. The FEA thus contains fairly complicated thermal staging to keep the 130 K FETs in close proximity to the 60 mK detectors while not contributing significantly to the parasitic heat load on the CTS and ADR. The FET thermal staging must also not contribute significantly to the lifetime of either the solid neon or helium cryogen tanks. This is described in more detail in section 3.2

The fully assembled FEA is mounted over the magnet bore in the helium tank that contains the ADR and is bolted directly to the helium tank at 1.3K. The top cover of the FEA contains the second of five infrared blocking filters completing the 1.3K thermal shield for the CTS and the ADR.

3.1 The Calorimeter Thermal Stage (CTS)

The Calorimeter Thermal Stage (CTS) is the temperature-controlled platform that houses the microcalorimeter array, an anti-coincidence detector and their associated load resistors. In addition, the CTS contains four RuO_2 thermistors that are the

redundant control and monitor thermometers for the ADR. The CTS's temperature is controlled at 60.00 mK with < 10 μ K rms noise by regulating the external magnetic field applied to the salt pill.

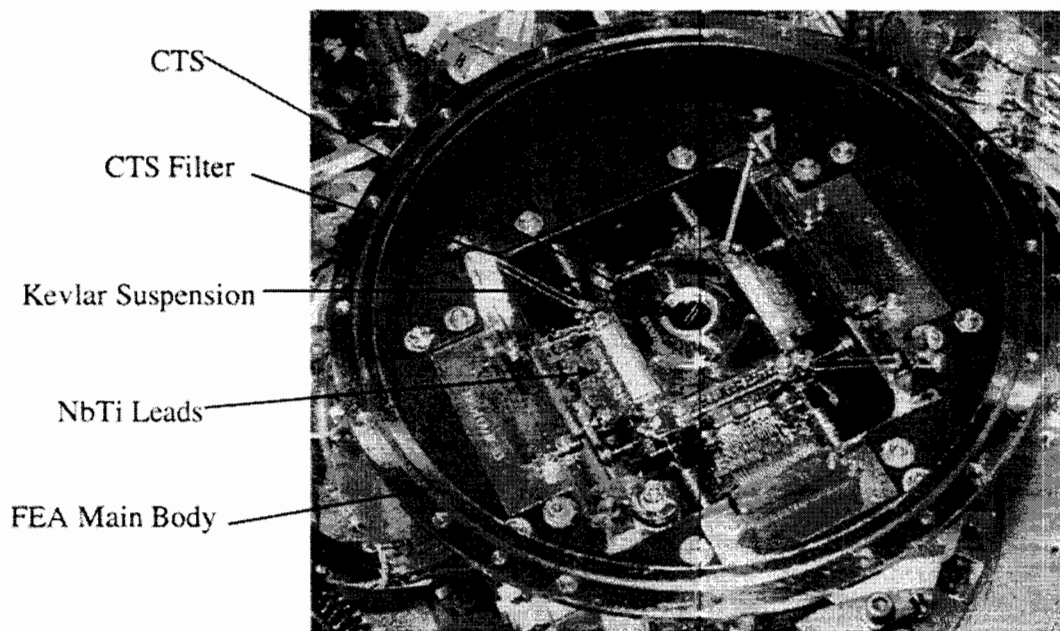


Figure 10. Top view of the XRS FEA with its cover removed. The CTS is shown suspended in the center of the FEA main body.

The microcalorimeter array is housed inside the CTS, with a tongue and groove lid to minimize stray light. The array is mounted on a high purity alumina board, backed by the anti-coincidence detector and wire bonded into the CTS. The electrical feedthroughs through the wall of the CTS are custom built alumina blocks which have a buried wire layer and are gold plated everywhere except for wire bond pads on the inside of the CTS and Be-Cu pins on the outside. The buried wiring layer contains two right angles so that there is no direct light path through the feedthroughs to the interior of the CTS. This is extremely important because the microcalorimeters also have a bolometric response and will be heated by any stray light entering the CTS, reducing their responsivity.

The underside of the CTS contains an alumina board holding the 90 M Ω load resistors, which are located at 60 mK to minimize Johnson noise. The lid of the CTS contains the first aluminum coated polyimide infrared blocking filter and also contains the small ^{55}Fe and ^{41}Ca x-ray calibration sources. The attachment to the ADR is made with four pairs of annealed high-purity gold foils which are clamped to the CTS and to the FEA bus of the salt pill (see section 2.3). The thermal conductivity of the CTS to the ADR is 0.14 mW/K. This gives a 1.7 mK drop to the salt pill thermal bus for the 0.24 μ W of parasitic heat input to the CTS. The gold foil thermal connection to the salt pill mechanically de-couples the CTS from the ADR allowing us to separately suspend the CTS and stage it at a higher resonance frequency.

The CTS is suspended from the outer housing of the FEA using 195 denier (1 denier = 1 gram/9 km) Kevlar 49 tensioned to 2.6 lbs. This gives the 70g CTS a resonant frequency between 300 and 350 Hz, well isolated from the 90 Hz dewar resonance and the \sim 200 Hz salt pill resonance. The Kevlar suspension contributes negligibly to the parasitic heat load on the ADR while providing a stiff support for the CTS. The CTS has maintained its alignment within the FEA to $< 0.001^\circ$ through both thermal cycling and vibration tests.

The CTS is wired to both the FET boxes (described in section 3.2) and the bias box using 20 μ m diameter CuNi clad NbTi wire. The use of superconducting wire minimizes the parasitic heat flow from the 1.3K connectors on the FEA to the 60 mK CTS. The superconducting wire is plated with a 0.8 μ m layer of 70% Cu, 30% Ni alloy making the wire easily solderable using standard rosin fluxes. All of the wires bridging the CTS to the FEA are "flying" leads, in that they are tensioned across the gap between the two components by spring loaded Be-Cu contacts. The wires are tensioned to 6–10g to boost the resonance frequency and the associated microphonic signal out of the detector bandpass (10 – \sim 400Hz). This is important for the microcalorimeters because the thermistor has a source impedance of 10 M Ω under its nominal bias. Thus the wiring up to the trans-impedance amplifier must be rigid to avoid microphonics. There are a total of 130 suspended and tensioned leads bridging the 1.3 K FEA housing to the CT, dominating the 0.3 μ W of parasitic heat load from the CTS to the ADR.

3.2 The FET Trans-impedance Amplifiers

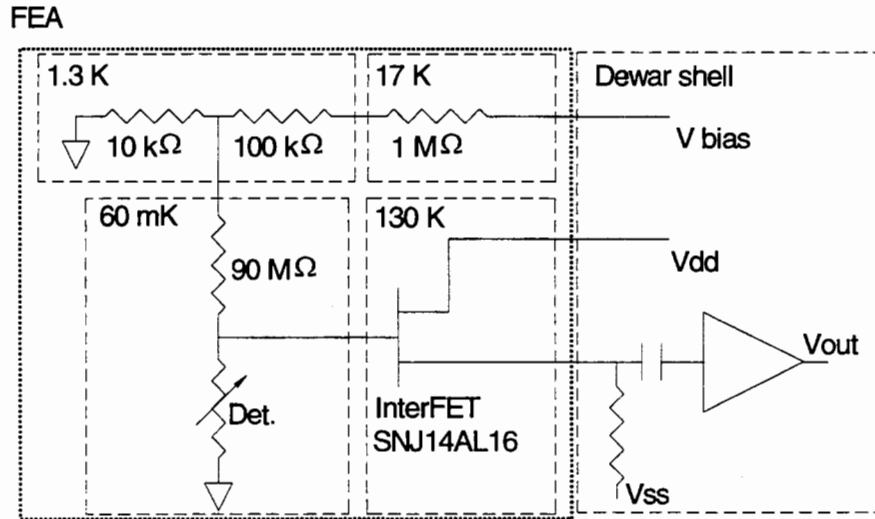


Figure 11. A schematic diagram of the detector read out circuit.

The FET stage itself presents a significant challenge in the design of a microcalorimeter instrument. While the detectors themselves must be run at very low temperatures. The FETs must be operated at a significantly higher temperature in order to keep the carriers in the silicon from freezing out. In the XRS, the FETs are temperature controlled at 130K which is near their noise minimum. In addition, the leads bridging between the detectors and the FETs must be rigid to avoid microphonics. The FETs must thus be placed in close proximity to the detectors, which complicates the thermal design.

The FETs used in the XRS are InterFET SNJ14AL16 that were supplied to us as bare die. We then characterized the FETs at 130K, choosing the lowest noise components for assembly into the FEA. The noise performance of the FETs in the flight assembly ranges from 3 to 5 nV/Hz^{1/2} at 100 Hz. The FET trans-impedance amplifiers reduce the 10 MΩ source impedance of the detectors to the 1.8 kΩ output impedance of the FETs substantially reducing any microphonic contamination of the detector signal.

The XRS FEA contains two separate FET assemblies to provide redundancy. The loss of one of the modular FET assemblies allows half of the detectors to continue to function. The assemblies are mated through high-density connectors to the FEA main section where tensioned electrical leads make connection to the CTS. The challenge inside the FET assemblies is to allow the FETs to operate at 130 K while minimizing the heat loads on both the helium and neon cryogenic tanks. To accomplish this, the FETs are doubly suspended inside nested copper boxes. The outer box is bolted to the FEA body and is thermally anchored at 1.3 K, while the inner box is thermally anchored to the neon tank at 17 K through a carefully routed thermal strap. The inner FET box is suspended by 195 denier Kevlar inside the outer FET box. Inside the inner FET box, the FETs themselves are organized into two separate packages of 9 FETs each (16 for the microcalorimeters, 1 for the anti-coincidence detector, and 1 spare). Each package also contains a diode thermometer and a heater for temperature control. The two packages are mounted on an aluminum substrate (totaling a few grams) that is then suspended with 55 denier Kevlar to the inner FET box. The FETs are thus effectively thermally isolated from the ADR, which has the lowest requirement for parasitic heat. The FET boxes do contribute 95 μW to the helium and 11 mW to the neon tank. Thus more than 99% of the power to run the FETs is shunted away from the helium tank.

The wiring in both the inner and outer FET boxes is 25 μm diameter CuNi clad stainless steel wire. The 1 μm 70% Cu, 30% Ni overcoat allows the wire to be soldered without using a highly corrosive flux. Stainless steel wire was chosen for its superior strength and low thermal conductivity. As on the CTS, the wiring in the FET boxes is tensioned to avoid microphonics in the detector bandpass.

Light leaks from the 130 K FETs are also a significant problem for the microcalorimeters and to some extent the ADR itself. To prevent long wavelength radiation from the FETs reaching the detectors, each FET box has a specially constructed electrical feedthrough. The feedthroughs are constructed using Eccosorb¹³ CR-117 which is an epoxy filled with iron fillings providing effective shielding from the hot FETs. We have not observed any stray power on the microcalorimeter detectors from any source associated with the FET amplifiers.

4. CONCLUSIONS

The XRS instrument currently defines the state-of-the-art in low temperature detector instrumentation for x-ray astrophysics. Once it is launched in early 2000, it will be the premier broadband x-ray spectrometer for several years to come. It contains the largest adiabatic demagnetization refrigerator ever built and will set the record for the lowest temperature ever achieved on an orbiting platform. However, the XRS is a very large instrument, dominating the Astro-E observatory in both size and weight. Future instruments will benefit from the extensive development experience from XRS.

Looking to the future, the Constellation-X mission contains the logical successor to XRS both in detector design and in cryogenic design. However, it will surpass and extend the XRS instrument in several important ways. The cryogen tanks will probably be replaced by compact, low vibration cryocoolers providing a 3-6 K heat sink for a multi-stage ADR. This will make the instrument much more compact with a lifetime no longer limited by stored cryogen tanks. The detector array should achieve a resolving power of 3000 at 6 keV and the 32 pixel XRS array will be expanded to a 900 pixel imaging microcalorimeter array. For a more detailed description of the future of low temperature detectors in x-ray astrophysics see Stahle *et al.*¹⁴ in this proceeding.

REFERENCES

1. Kevlar is a registered trademark of the Du Pont Company.
2. R. L. Kelley, M. D. Audley, K.R. Boyce, S. R. Breon, R. Fujimoto, K.C. Gendreau, S. S. Holt, Y. Ishisaki, D. McCammon, T. Mihara, K. Mitsuda, S. H. Moseley, B. Mott, F. S. Porter, C. K. Stahle, "The Astro-E/XRS high resolution spectrometer," in *Proc. SPIE*, **3765**, 1999.
3. S. Deiker, R. Kelley, A. Lesser, D. McCammon, F.S. Porter, W.T. Sanders, C.K. Stahle, and A.E. Szymkowiak, "First Results from a Suborbital Flight of a 36 Pixel Microcalorimeter Array," in *Proc. Low Temperature Detectors 7*, pp 108-114, 1997.
4. S. R. Breon, M. J. Dipirro, J. G. Tuttle, P. J. Shirron, B. A. Warner, R. F. Boyle and E. R. Canavan, "Thermal Performance of the XRS Helium Cryostat," to appear in *Advances in Cryogenic Engineering*, **44**, 1999.
5. M. D. Audley, K. A. Arnaud, K. C. Gendreau, K. R. Boyce, C. M. Fleetwood, R. L. Kelley, R. A. Keski-Kuha, F. S. Porter, C. K. Stahle, A. E. Szymkowiak, J. L. Tveekrem, R. Fujimoto, K. Mitsuda, Y. Ishisaki, and T. Mihara, "Astro-E/XRS Blocking Filter Calibration," in *Proc. SPIE*, **3765**, 1999.
6. E. Mendoza, "Magnetic Cooling". *Experimental Cryophysics*, pp 165-213, 1961.
7. O. E. Vilches and J. C. Wheatley, "Measurements of the Specific Heats of Three Magnetic Salts at Low Temperatures," *Phys. Rev.*, **148**, pp 509-516, 1966.
8. Vespel is a registered trademark of the Du Pont company.
9. The TI-15333 alloy is available, for example, from the Timet company, Denver, CO.
10. ScotchWeld is a registered trademark of the 3M company.
11. C. Hagmann, D. J. Benford, and P. L. Richards, "Paramagnetic salt pill design for magnetic refrigerators used in space applications," *Cryogenics*, **34**, pp 213-219, 1994.
12. C. Hagmann and P.L. Richards, "Specific Heat of Stainless Steel below T=1K," *Cryogenics*, **35**, p. 345, 1995.
13. Eccosorb is a registered trademark of the Emmerson and Cummings company.
14. C. K. Stahle, S. R. Bandler, T. Barbee Jr., J. Beeman, R. P. Brekosky, B. Cabrera, M. Cunningham, S. Deiker, E. Figueroa-Feliciano, F. M. Finkbeiner, M. Frank, K. C. Gendreau, E. E. Haller, G. C. Hilton, K. D. Irwin, R. L. Kelley, S. E. Labov, M. J. Li, N. Madden, J. M. Martinis, D. McCammon, S. Nam, F. S. Porter, H. Schnopper, E. H. Silver, A. E. Szymkowiak, G. S. Tucker, A. Walker, D. A. Wollman, "Toward a 2-eV Microcalorimeter X-ray Spectrometer for Constellation-X," in *Proc. SPIE*, **3765**, 1999.